Intraseasonal Surface Fluxes in the Tropical Western Pacific and Indian Oceans from NCEP Reanalyses

TOSHIAKI SHINODA, HARRY H. HENDON, AND JOHN GLICK

Climate Diagnostics Center, University of Colorado, Boulder, Colorado

(Manuscript received 23 December 1997, in final form 18 May 1998)

ABSTRACT

Reliability of the surface fluxes from National Centers for Environmental Prediction (NCEP) reanalyses is assessed across the warm pool of the western Pacific and Indian Oceans. Emphasis is given to the spatial distribution and coherence of the fluxes on intraseasonal (25–100 day) periods, as intraseasonal variability predominates the subseasonal variability across the warm pool. Comparison is made with surface fluxes estimated from data collected at a mooring during the Coupled Ocean–Atmosphere Response Experiment and with independent gridded estimates based on operational wind and surface pressure analyses and satellite observations of rainfall, shortwave radiation, and outgoing longwave radiation. In general, fluxes that depend primarily on surface wind variations (e.g., stress and latent heat flux) agree more favorably than fluxes that are largely dependent on fluctuations of convection (e.g., surface shortwave radiation and freshwater or precipitation). In particular, the intraseasonal variance of shortwave radiation and precipitation in the NCEP reanalyses is about half of that estimated from in situ observations and from satellite observations. Composite surface flux variations for the Madden–Julian oscillation, which is the dominant mode of intraseasonal variability in the warm pool, are also constructed. Again, the composite variations of wind stress and latent heat flux from the NCEP reanalyses agree reasonably well, both in magnitude and phasing, with the composite fluxes from the independent gridded data. However, the composite intraseasonal shortwave radiation and precipitation from the NCEP reanalyses, while agreeing in phase, exhibit less than half the amplitude of the satellite-based estimates.

The impact of the underestimation of these surface flux variations in the NCEP reanalyses on the intraseasonal evolution of sea surface temperature (SST) in the warm pool is investigated in the context of a one-dimensional mixed layer model. When forced with the intraseasonal surface fluxes from the NCEP reanalyses, the amplitude of the intraseasonal SST variation is some 30%–40% smaller than observed or than that from forcing with the independent gridded fluxes. This reduced amplitude is primarily caused by the underestimation of the intraseasonal shortwave radiation variations in the NCEP reanalyses.

1. Introduction

The National Centers for Environmental Prediction (NCEP), in collaboration with the National Center for Atmospheric Research (NCAR), have produced 40 yr of reanalysis of global atmospheric fields using a frozen state-of-the-art global assimilation system (Kalnay et al. 1996). The input database includes many observations not available in real time. Hence, the reanalysis has many potential benefits over real-time analyses generated in support of operational weather prediction, which have been used in a wide range of research during the last two decades. However, many fields provided from the reanalysis depend, to a varying degree, on the parameterized physics of the global circulation model employed in the assimilation system. Included in such fields are surface fluxes of momentum, heat, radiation, and freshwater. Such fluxes have many potential uses including forcing ocean circulation models and ingesting into ocean data assimilation systems. Evaluation of the quality of the surface fluxes provided by reanalysis is thus required, both for aiding improvements to future reanalysis efforts and for guidance in their current usage.

Some aspects of the reliability of the surface fluxes from reanalysis have been recently examined by Bony et al. (1997), who compared surface fluxes from the NCEP reanalyses with estimates from satellite and in situ data collected over the tropical oceans. They found that the net surface heat flux from the NCEP reanalyses can differ from these other estimates by up to 50 W m^{-2} in the mean and by a factor of 2 when considering interannual anomalies. Weare (1997) compared net downward shortwave radiation at the surface from the NCEP analyses with estimates by Li and Leighton (1993), which are derived from Earth Radiation Budget Experiment data and European Centre for Medium-Range Forecasts (ECMWF) humidity data. They found

Corresponding author address: Dr. Toshiaki Shinoda, Climate Diagnostics Center, University of Colorado, Campus Box 449, Boulder, CO 80309.
E-mail: ts@cdc.noaa.gov

significant differences across the tropical oceans (20–30 W m^{-2}) and attributed them to shortcomings of the shortwave cloud forcing produced by the reanalysis model. These studies focused on seasonal and interannual timescales, whereas evaluation of the NCEP surface fluxes at shorter timescales has not been provided.

The focus of the present study is on depiction of surface flux variation in the NCEP analyses across the warmest waters of the tropical Indian and Pacific Oceans (the so-called warm pool) at intraseasonal timescales. Such a focus is motivated by the Coupled Ocean–Atmosphere Response Experiment (COARE) field program (Webster and Lukas 1992), which endeavored to understand the coupling of the atmosphere and ocean in the Pacific warm pool. A principal finding from COARE is that the sea surface temperature (SST) in the Pacific warm pool evolves systematically at an intraseasonal period of 30–60 days in association with variations of the surface flux of heat and momentum (e.g., Weller and Anderson 1996; Lau and Sui 1997). Subsequent studies have shown these intraseasonal variations of SST and surface fluxes to have large spatial coherence (i.e., ≈10 000 km), to propagate eastward, and to be detectable from the western Indian Ocean eastward past the date line (e.g., Hendon and Glick 1997; Shinoda et al. 1998, hereafter SHG98). There is growing evidence that these intraseasonal variations of surface fluxes play an important role in the maintenance of the warm pool (e.g., Ralph et al. 1997) and possibly in eastward displacements of the eastern edge of the warm pool in the Pacific (e.g., Kessler et al. 1995). Hence, knowledge of the reliability of the intraseasonal surface fluxes from the NCEP reanalyses is desirable so that such behavior might possibly be studied with the long, continuous record afforded by the reanalysis effort.

In the present study, surface fluxes from the NCEP reanalyses will be compared with accurate point estimates from a mooring deployed during COARE (Weller and Anderson 1996) and with the gridded estimates produced by SHG98, which cover the entire warm pool. In both cases, the comparison focuses on the structure and coherence of the fluxes for periods 35–85 days, which is where the intraseasonal power in surface winds and convection is concentrated across the warm pool (e.g., Salby and Hendon 1994). SHG98 also constructed a composite of the surface flux variation associated with the Madden–Julian oscillation (MJO; Madden and Julian 1971, 1972), which is the dominant mode of intraseasonal variability across the warm pool. A similar composite will be made here using the NCEP fluxes in order to assess the ability of the reanalysis to depict this large-scale intraseasonal mode. Also, in order to quantify the impact of surface flux errors on the intraseasonal evolution of SST in the warm pool, a one-dimensional mixed-layer model is integrated using the NCEP fluxes and compared to similar integrations reported in Shinoda and Hendon (1998).

This paper is organized as follows: spectral analyses and horizontal distributions of intraseasonal variance using NCEP fluxes and the fluxes produced by SHG98 are presented in section 2. Comparison is also made with the accurate point estimates from the Improved Meteorological Instrument (IMET) mooring deployed in the equatorial western Pacific during COARE (Weller and Anderson 1996). Composites of the surface fluxes for the MJO are discussed in section 3. Section 4 presents the mixed layer modeling using NCEP surface fluxes, and conclusions are stated in section 5.

2. Comparison of intraseasonal surface fluxes and convection

In this section, the spectral characteristics and intraseasonal variance of surface winds and fluxes provided by the NCEP reanalysis are examined. Comparison is made with surface winds and fluxes from a variety of sources. These include the uninitialized wind analyses from ECMWF, daily precipitation from the microwave sounding unit (MSU; Spencer 1993), and the surface flux estimates produced by SHG98 (described below). Net shortwave radiation at the surface, which is derived from daily estimates of downwelling shortwave radiation produced by Pinker and Laszlo (1992) as part of the Surface Radiation Budget Project (Whitlock et al. 1995), is also used for the comparison. We will refer to this net shortwave radiation estimate as SRB. Together with these surface fields, top of the atmosphere outgoing longwave radiation (OLR) is also examined, as OLR is a useful proxy for depicting the important convective fluctuations associated with tropical intraseasonal variability over the warm pool. For comparison with the model generated OLR from the NCEP reanalysis, we use the satellite-based OLR dataset prepared by Liebmann and Smith (1996), which is based on twice daily estimates of OLR described by Gruber and Krueger (1984). Hereafter, we will refer to this data as satellite-based OLR. Fields from NCEP reanalyses are interpolated onto 2.5° × 2.5° grid to be compatible with these other fields and the flux estimates provided by SHG98. Daily averages of the flux estimates for the 7-yr period July 1986 to June 1993 are used for the comparison (except for comparison with SRB data, which is limited to 1985–88).

The surface fluxes produced by SHG98, which are used for comparison with the NCEP reanalyses, are briefly described here. SHG98 estimated momentum and heat fluxes at the surface using uninitialized analyses of winds and surface pressure from ECMWF and satellite-based OLR. Net shortwave radiation is estimated from satellite-based OLR based on a linear regression of OLR onto the available daily SRB data. Latent and sensible heat fluxes and wind stress are estimated using daily ECMWF winds along with weekly SST analyses (Reynolds and Smith 1994) and empirical estimates of air temperature and specific humidity based on SST as giv-

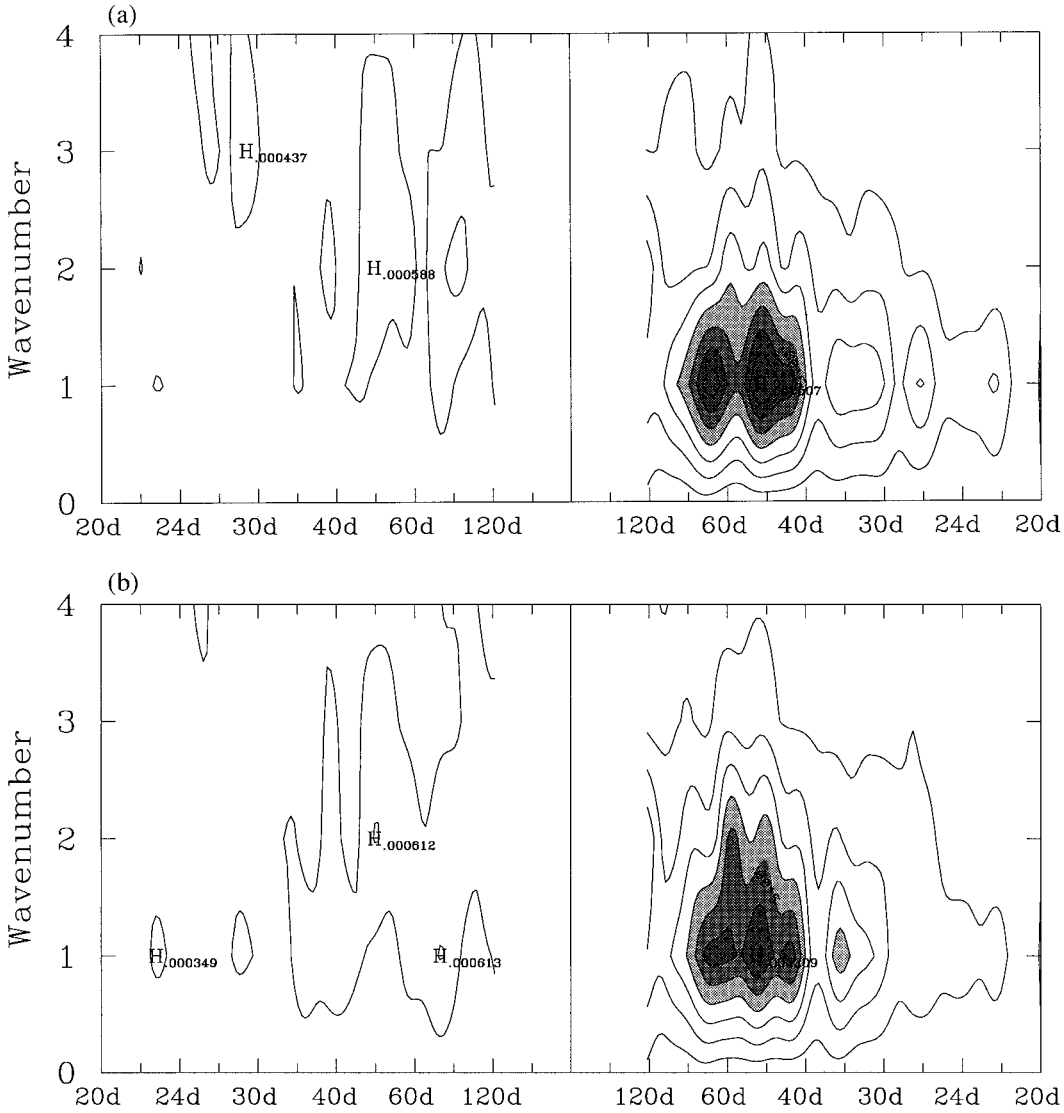

FIG. 1. Space–time power spectra for 1000-mb zonal winds from (a) NCEP reanalyses and (b) uninitialized ECMWF analyses for the period 1 July 1986–30 June 1993. Contour interval is 0.0003 $m^2 s^{-2}$. Values greater than 0.0012 $m^2 s^{-2}$ are shaded. The right half and left half of the figures indicate eastward and westward propagation, respectively. The spectra at each wavenumber were smoothed with successive passes of a three-frequency running average such that the effective bandwidth is increased from its nominal value of 1/2555 cycles per day to 8/2555 cycles per day.

en by Waliser and Graham (1993). The Tropical Ocean Global Atmosphere (TOGA) COARE bulk flux algorithm (Fairall et al. 1996) is then used to estimate these fluxes. Net longwave radiation is estimated using the formula of Berliand and Berliand (1952) along with specific humidity and air temperature from the formula by Waliser and Graham (1993), the weekly SST analyses, sea level pressure from ECMWF analyses, and total cloudiness obtained from a regression analysis between satellite-based OLR and total cloudiness from International Satellite Cloud Climatology Project data (Rossow and Schiffer 1991). SHG98 showed that these flux estimates agree reasonably well with the estimates from the IMET mooring data collected during TOGA COARE, particularly at intraseasonal timescales (see SHG98 for more detail).

Assessment of the reliability of the NCEP surface fluxes at intraseasonal timescales begins with examination of wavenumber–frequency spectra of the 1000-mb zonal wind (Fig. 1) and OLR (Fig. 2). These spectra are calculated by Fourier transform technique using the 7-yr record (1 July 1986–30 June 1993). Prior to spectral transform, the time series are tapered with a cosine-rectangular window over the first and last 5% and averaged between 7.5°N and 7.5°S. Since this analysis focuses on 35–85-day periods, the spectrum for periods less than 20 days and more than 120 days are not shown in Figs. 1 and 2. Note that wavenumbers shown in Figs.

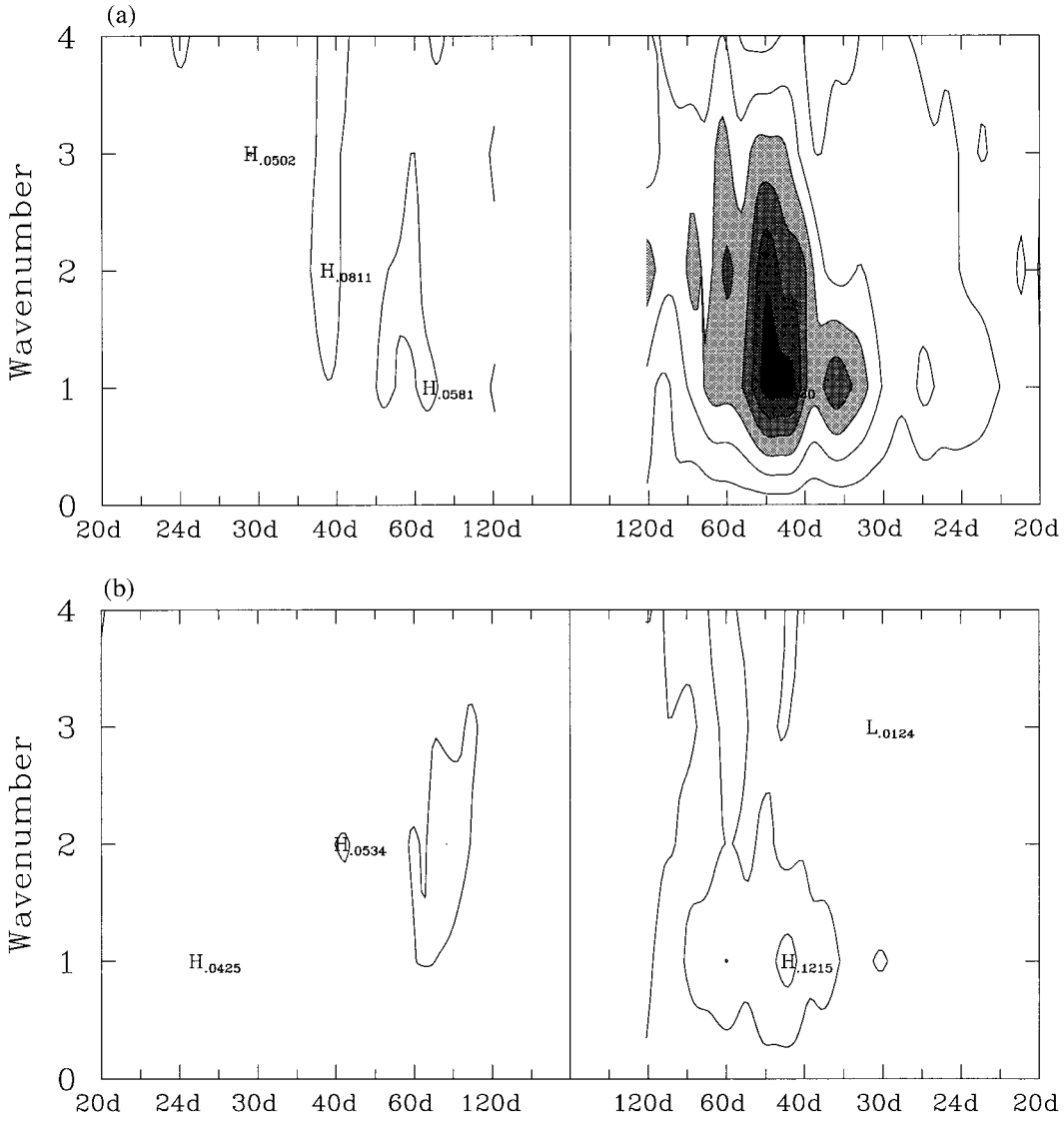

FIG. 2. Space–time power spectra for (a) satellite-derived OLR and (b) OLR from NCEP reanalyses. Plotting convention and computation of spectra are as in Fig. 1. Contour interval is 0.05 W^2 m^{-4}. Values greater than 0.15 W^2 m^{-4} are shaded.

1 and 2 are global wavenumber since the data from entire longitudes are used to compute the spectrum.

The spectrum of 1000-mb zonal wind from the NCEP reanalyses displays the familiar broad spectral peak at 40–60 days for eastward wavenumber 1 (Fig. 1a), which is indicative of the MJO (e.g., Salby and Hendon 1994). A similar spectral peak is found in the ECMWF 1000-mb zonal wind (Fig. 1b), but is slightly broader in wavenumbers 1–3. The sharper peak at wavenumber 1 in the NCEP analyses is indicative that the horizontal distribution of intraseasonal variance is not as spatially confined across the Indian and western Pacific Oceans as that in the ECMWF analyses [see Salby and Hendon (1994) and below for further discussion]. Nonetheless, the zonal wind spectra are sufficiently similar to conclude that both analyses depict similar behavior for the dominant eastward propagating intraseasonal mode in surface zonal wind.

On the other hand, examination of the spectra of OLR (Fig. 2) indicates that the NCEP analyses are woefully inadequate at these eastward intraseasonal periods. Whereas the observed OLR possesses a strong concentration of power at intraseasonal periods around 40–50 days for eastward wavenumbers 1–3, the NCEP OLR at these wavenumbers and periods is roughly a factor of 6 smaller. This suggests that the convective activity associated with the MJO is not well captured by the NCEP reanalyses, despite the fact that a clear dynamical signal is present (Fig. 1).

Such a deficiency in intraseasonal convective vari-

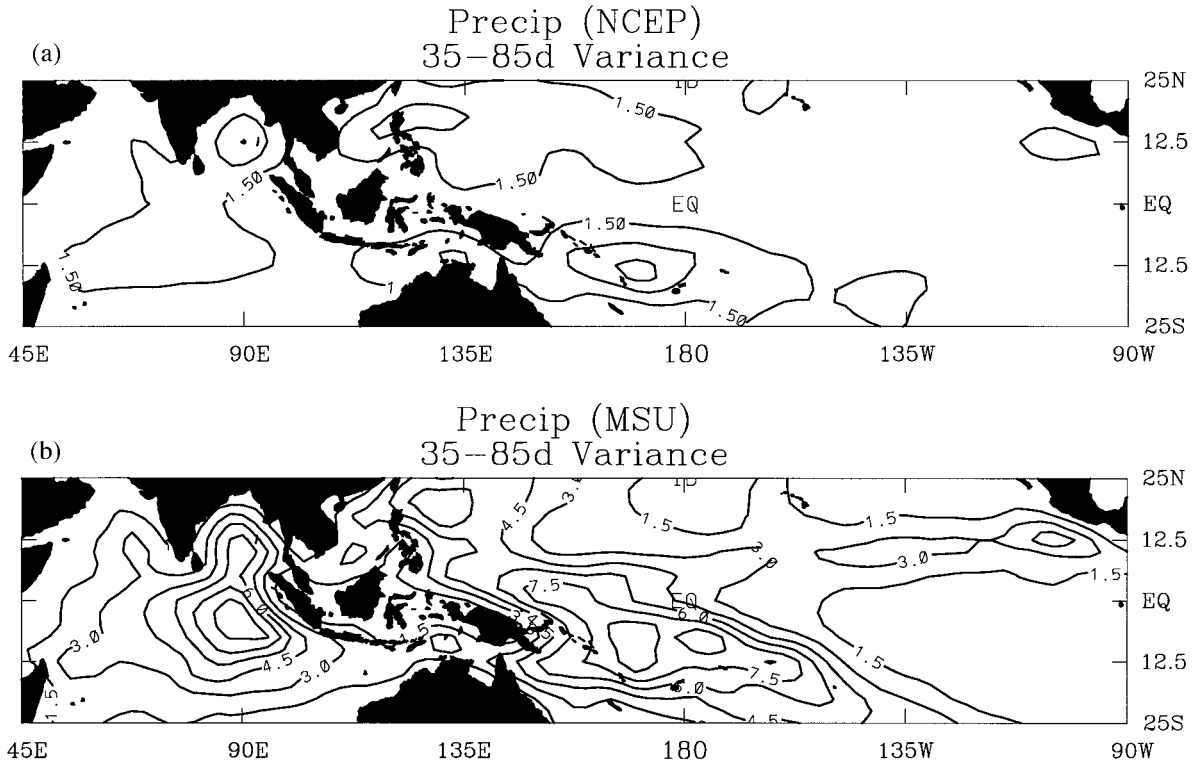

FIG. 3. Variance of intraseasonally filtered (35–85-day period) precipitation ($mm^2\ day^{-2}$) from (a) NCEP reanalyses and (b) MSU, for the period 1 July 1986–30 June 1993.

ance is also reflected in other fields that are intimately related to convection, such as rainfall and surface shortwave radiation. For instance, the horizontal distribution of intraseasonal (35–85 day) rainfall variance is shown in Fig. 3. Whereas the distribution of NCEP rainfall variance is spatially bland, with only a weak maximum south of the equator in the western Pacific, the microwave sounding unit (MSU) rainfall variance exhibits two pronounced maxima, one in the equatorial Indian Ocean and one in the western Pacific, both of which are ≈6 times stronger than that from NCEP. Similar differences exist between SRB and NCEP surface shortwave radiation and satellite-based OLR and NCEP OLR (not shown).

The above analysis suggests that intraseasonal surface fluxes from NCEP reanalyses and SHG98 will agree more favorably for those fluxes that predominantly depend on surface winds (e.g., stress and latent heat flux) than do those that depend strongly on variations of convection (e.g., surface shortwave radiation and rainfall). Such a conclusion is confirmed by considering the coherence squared and ratio of the square root of intraseasonal variances (hereafter the ratio of intraseasonal amplitudes) for a number of surface fluxes from NCEP reanalyses and SHG98. The ratio of intraseasonal amplitudes for zonal wind stress (Fig. 4a) is very close to 1 (0.9–1.1) across the entire equatorial Indian and western Pacific warm pool. The coherence squared exceeds 0.7 across the entire equatorial warm pool, indicating that very little difference exists between these two estimates. A large difference is evident in the South Pacific convergence zone near the date line. The reason for this difference is not known. The ratio of intraseasonal amplitude for latent heat flux (Fig. 4b) is also close to 1 across the equatorial warm pool, but the NCEP estimates are systematically larger at higher latitudes (poleward of 10°). A part of the reason for this could be the difference of specific humidity variance. The intraseasonal amplitude of the difference between saturated specific humidity at the surface and air specific humidity in the NCEP reanalyses is systematically larger at higher latitude than that from the estimate by the Waliser and Graham (1993) formula (not shown), which is used by SHG98 in their estimate of the latent heat flux. Note that the empirical formula by Waliser and Graham (1993) is derived from the satellite data in the western equatorial Pacifc. Hence the validity of the formula in other regions is uncertain, and comparison at higher latitude may not be appropriate. The larger intraseasonal amplitude for the NCEP latent flux at higher latitudes could also be due to the NCEP bulk flux algorithm. Zeng et al. (1998) indicated that the NCEP algorithm produced significantly larger latent heat flux at high wind speed compared to the estimate from the COARE bulk flux algorithm and to observed values, but reasonable agreement under low wind conditions. Their find-

ing is consistent with the behavior seen in Fig. 4b, as the agreement is better near the equator where the winds are weak, whereas the NCEP estimates are larger off the equator where the trade winds are stronger. Although the coherence squared is large (≈0.7) across the warm pool, it is slightly weaker than that for stress. Such a reduction is expected because of the contribution (though relatively weak; e.g., Zhang 1996) by humidity fluctuations to the intraseasonal latent heat flux variations, which are largely absent in the SHG98 estimates and of unknown quality in the NCEP reanalyses.

The ratio of intraseasonal amplitude of precipitation and surface shortwave radiation and their coherence squared are shown in Figs. 4c and 4d, respectively. As expected from Fig. 2, the intraseasonal amplitude of precipitation from the NCEP reanalyses is about one-half that of the MSU precipitation across the warm pool.[1] Furthermore, intraseasonal variations of precipitation depicted in the NCEP reanalyses are largely incoherent with those depicted by the MSU (i.e., the coherence squared is less than 0.3 across large regions of the warm pool). The intraseasonal amplitude of the NCEP shortwave radiation is also roughly half that of SRB and the coherence squared is less than 0.3 across large regions of the warm pool. Similar behavior is found for OLR (not shown). The comparison of the NCEP net surface longwave radiation with the estimate by SHG98 is shown in Fig. 4e. Across the bulk of the warm pool the NCEP estimate is slightly larger than that from SHG98 (amplitude ratio 1.2 to 1.4) and the coherence squared is 0.5–0.7. Outside of the equatorial warm pool region, the agreement is much worse. However, the estimates from SHG98 are not deemed reliable outside of this region due to their use of OLR to estimate total cloudiness for input into the empirical formula for net longwave radiation. Fluctuations of total cloudiness only can be inferred from OLR in regions of deep convection.

The above results indicate that while the NCEP reanalyses appear to reasonably depict the predominant large-scale wind variance at intraseasonal timescales, problems exist with those fields and fluxes related to intraseasonal convective variability (e.g., OLR, precipitation, and surface shortwave radiation). Further quantification of these inadequacies is provided in the following section by comparison to point estimates during COARE, which are considered to be relatively accurate for the intraseasonal timescale.

Data collected from the IMET mooring, which was deployed at 1°45′S, 156°E during COARE (22 October 1992–2 March 1993) were by used Weller and Anderson (1996) to estimate all components of the surface heat flux. The NCEP surface fluxes from the grid point centered at 2.5°S, 155°E are used for the comparison with these accurate point estimates. The estimates from the IMET mooring are especially germane to this study of intraseasonal fluxes because three eastward propagating, intraseasonal convective events passed across the IMET mooring during COARE (e.g., Gutzler et al. 1994). These intraseasonal convective events are interpreted as manifestations of the MJO (see also Hendon and Glick 1997). The first event occurred in late October 1992, the second (and much stronger event) in late December 1992, and the third in early February 1993.

The net surface shortwave and longwave radiation from the IMET measurements and NCEP reanalyses for the COARE period are shown in Figs. 5a and 5b, respectively. Although a clear intraseasonal variation of shortwave radiation, associated with the passage of the three aforementioned intraseasonal convective events, is evident in the IMET data, there is almost no signal in the NCEP reanalyses. The small intraseasonal variation in the NCEP estimate is consistent with the much reduced intraseasonal variance indicated in Fig. 4d. The intraseasonal variation of net surface longwave radiation observed at the IMET is not evident in the NCEP reanalyses either. The net surface longwave radiation from the NCEP reanalyses is also consistently smaller than that from the IMET. The difference sometimes exceeds 20 W m^{-2} during the calm/clear intraseasonal phases (e.g., late November–early December).

Figure 5c shows the comparison of the magnitude of the wind stress. As anticipated from Fig. 4a, wind stress from the NCEP reanalyses agrees well with the estimate from the IMET for intraseasonal timescales, as well as for shorter timescales. In particular, the large wind event in late December is well captured by the NCEP analyses, although the peak value is about 0.01 N m^{-2} higher than the IMET estimate. The latent heat flux estimates are shown in Fig. 5d. The intraseasonal variation is evident in both the NCEP reanalyses and the IMET estimate. However, during the strong wind event (late December), the NCEP estimate is significantly higher than the IMET estimate. The maximum value of the NCEP analyses in late December is, in fact, about 60 W m^{-2} larger. Under low wind conditions, the NCEP latent heat flux agrees reasonably well with the IMET estimate. As a result, the amplitude of intraseasonal variation of the NCEP latent heat flux is larger than that of the IMET estimate. The mean latent heat flux from NCEP analyses is about 10 W m^{-2} higher than the IMET estimate. This difference is possibly caused by the NCEP humidity and 2-m air temperature being systematically about 1°C cooler than the IMET estimate, which also causes about 9 W m^{-2} increase for the mean NCEP sensible heat flux (not shown).

The net surface heat flux (Fig. 5e) based on NCEP estimates is lower (more cooling) most of the time, although the amplitude of the intraseasonal variation agrees reasonably well. However, this agreement in am-

[1] The larger amplitude of the NCEP rainfall in the south eastern Pacific reflects an unrealistic double ITCZ structure produced in the reanalysis model. Note that the coherence squared is less than 0.1 in this region.

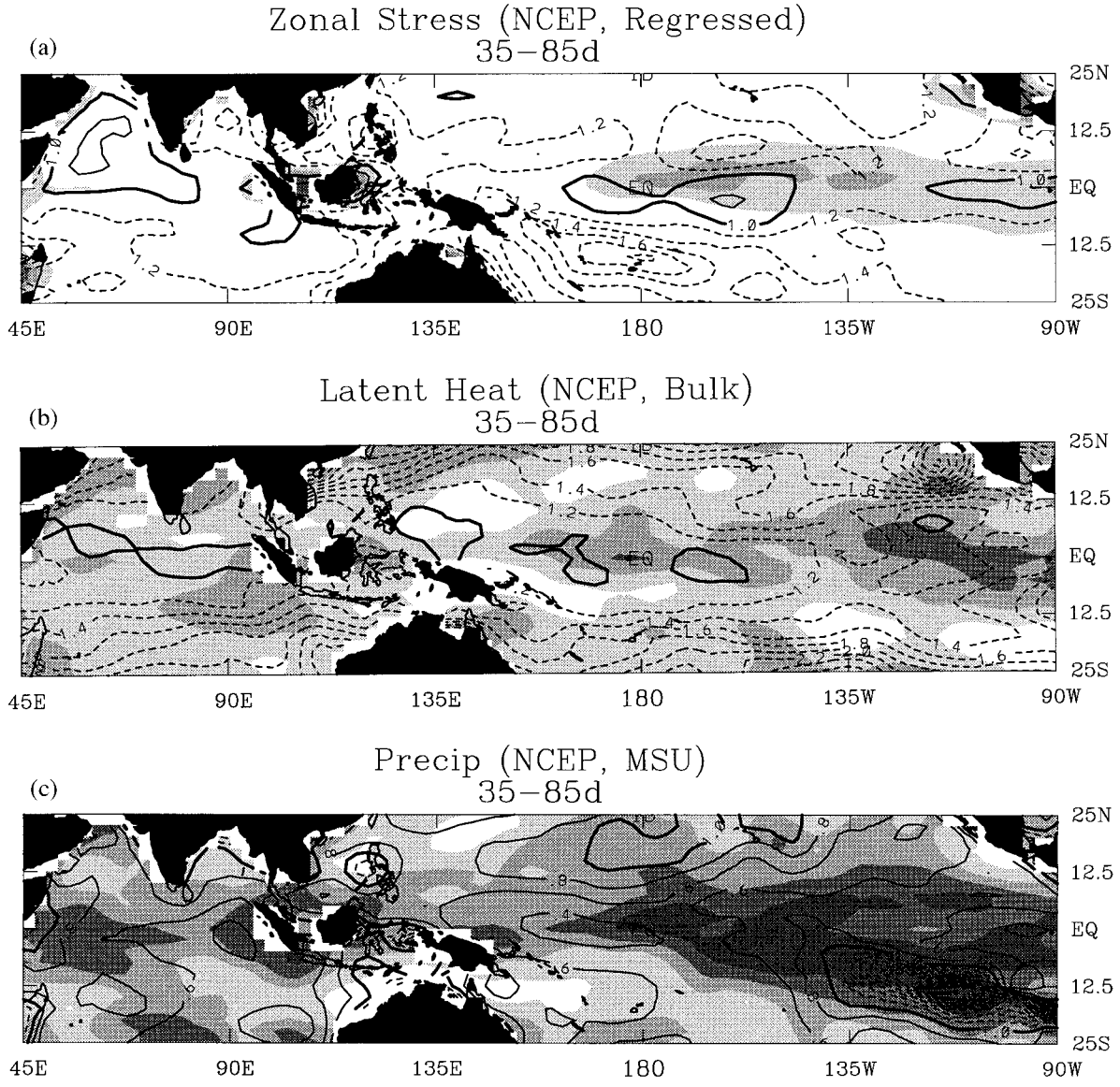

FIG. 4. (a) Ratio of the square root of intraseasonal (35–85-day period) variance of wind stress from NCEP reanalyses to that from SHG98 (contours) and the coherence squared between them in the 35–85-day band (shading). The contour interval is 0.2, with values greater than 1 (NCEP variance greater than SHG98 variance) dotted. Shading levels for coherence squared begin at 0.7, 0.5, 0.3, and 0.1. No shading

plitude for the intraseasonal variation of net surface heat flux results because the much weakened intraseasonal variation of net shortwave radiation in the NCEP reanalyses is compensated by a larger latent heat flux variation. Also, the smaller variation of the NCEP longwave radiation contributes to the compensation. As will be argued below, this cancellation is somewhat fortuitous and, in general, the amplitude of intraseasonal variations of net surface heat flux across the warm pool are underestimated in the NCEP reanalyses, due largely to underestimation of surface shortwave radiation fluctuations.

The comparison of the precipitation estimates is shown in Fig. 5f. Heavy precipitation during the windy phase/wet intraseasonal phase in late December is not evident in the NCEP analyses. The lack of this large intraseasonal rainfall variation is consistent with the lack of a similar fluctuation in net surface shortwave radiation, and again indicates a deficiency in the ability of the NCEP reanalyses to depict intraseasonal convective activity.

3. Comparison of MJO composites

The comparison with the fluxes from the IMET mooring for the COARE period has provided some insight into the depiction by the NCEP reanalyses of the surface flux variations produced by the MJO. However, no in-

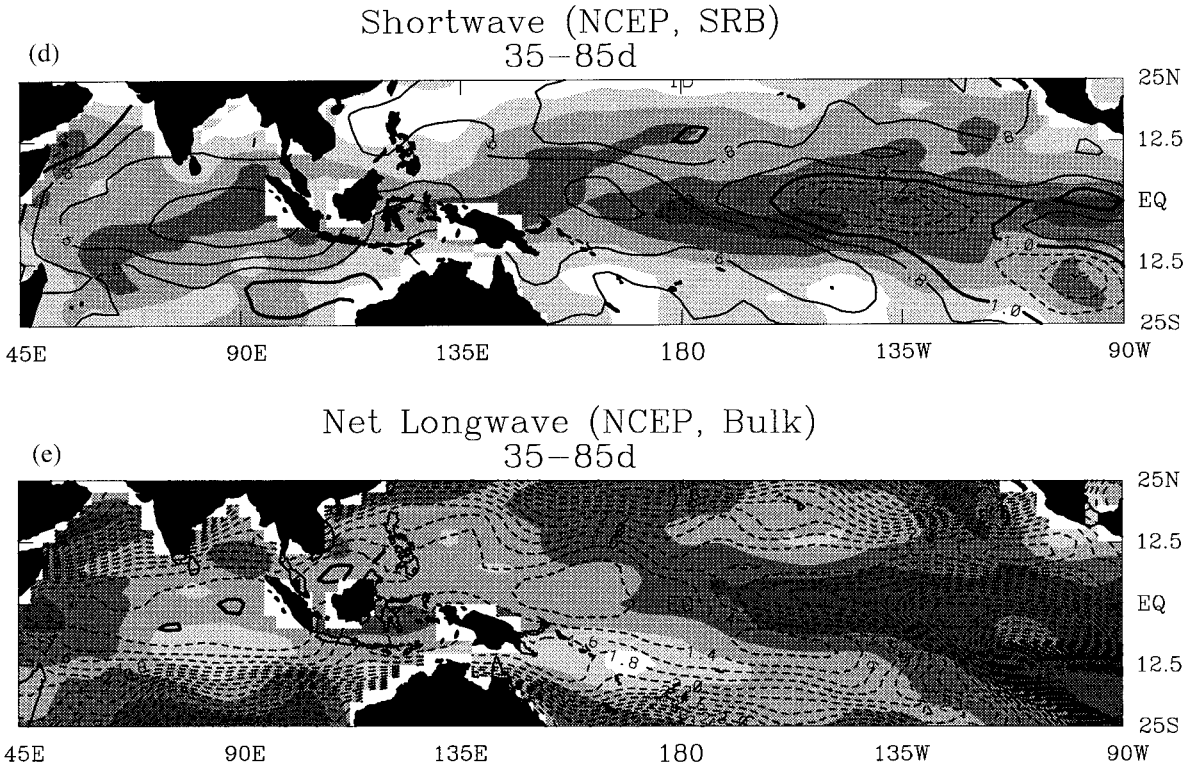

FIG. 4. (*Continued*) indicates that the coherence squared exceeds 0.7. (b) As in (a) except for latent heat flux from NCEP reanalyses and from SHG98. (c) As in (a) except for precipitation from NCEP reanalyses and MSU. (d) As in (a) except for shortwave radiation from NCEP reanalyses and that from SRB data. (e) As in (a) except for net surface longwave radiation from NCEP reanalyses and from SHG98.

formation about the spatial structure or eastward propagation of the fluxes produced by the MJO is provided by that comparison at a single point. To gain further insight into the depiction by the NCEP reanalyses of the surface flux variations associated with the dominant mode of intraseasonal variability across the warm pool, a composite for the MJO is constructed. Emphasis is given to not only the magnitude but also the relative phasing of the surface fluxes, which is known to be important for the SST anomalies generated by the MJO (e.g., Shinoda and Hendon 1998). The composite is constructed for 10 well-defined MJO events during 1986–93, as described in SHG98. These MJO events were identified based on EOF analyses of OLR and mostly occur during austral summer. In constructing the composite, all component surface fluxes are averaged onto a 5° lat × 10° long grid to emphasize the large-scale structure of the MJO. Further details of the compositing technique are found in SHG98.

The composite net surface shortwave radiation and zonal stress anomalies from the NCEP reanalyses and from the estimates by SHG98 are shown in Fig. 6. The vertical axis indicates temporal phase, where one cycle is approximately 50 days. The phase −90° corresponds to when minimum OLR, and thus the windy and wet phase of MJO, is in the western Pacific (see SHG98 for details). The shortwave radiation based on regression from observed OLR shows that the composite MJO systematically propagates eastward across the entire warm pool, with reduced insolation (increased convection) leading westerly stress by ≈5 days (Fig. 6b). The amplitude of the shortwave radiation fluctuation increases to the east from about 10 to 15 W m^{-2} in the Indian Ocean to about 30 W m^{-2} in the western Pacific. Only a hint of this eastward propagation is evident west of about 130°E in the NCEP shortwave radiation (Fig. 6a), whereas in the western Pacific, where some indication of eastward propagation is evident, the amplitude is about half that in Fig. 6b. On the other hand, the evolution of the composite zonal stress (both amplitude and phase) is nearly identical across the entire warm pool in the two estimates.

A more detailed comparison of the individual flux components is provided at 5°S, 165°E, which is representative of open ocean conditions in the western Pacific and where some semblance of the convective component of the MJO is evident in the NCEP reanalyses. The composite shortwave radiation is shown in Fig. 7. As expected from Fig. 6, the amplitude of intraseasonal variation from NCEP is about half that of the observed, and the mean value over the composite is about 15 W m^{-2} higher from the NCEP estimate.

The composite net surface longwave radiation is shown in Fig. 7b. The amplitude of the intraseasonal

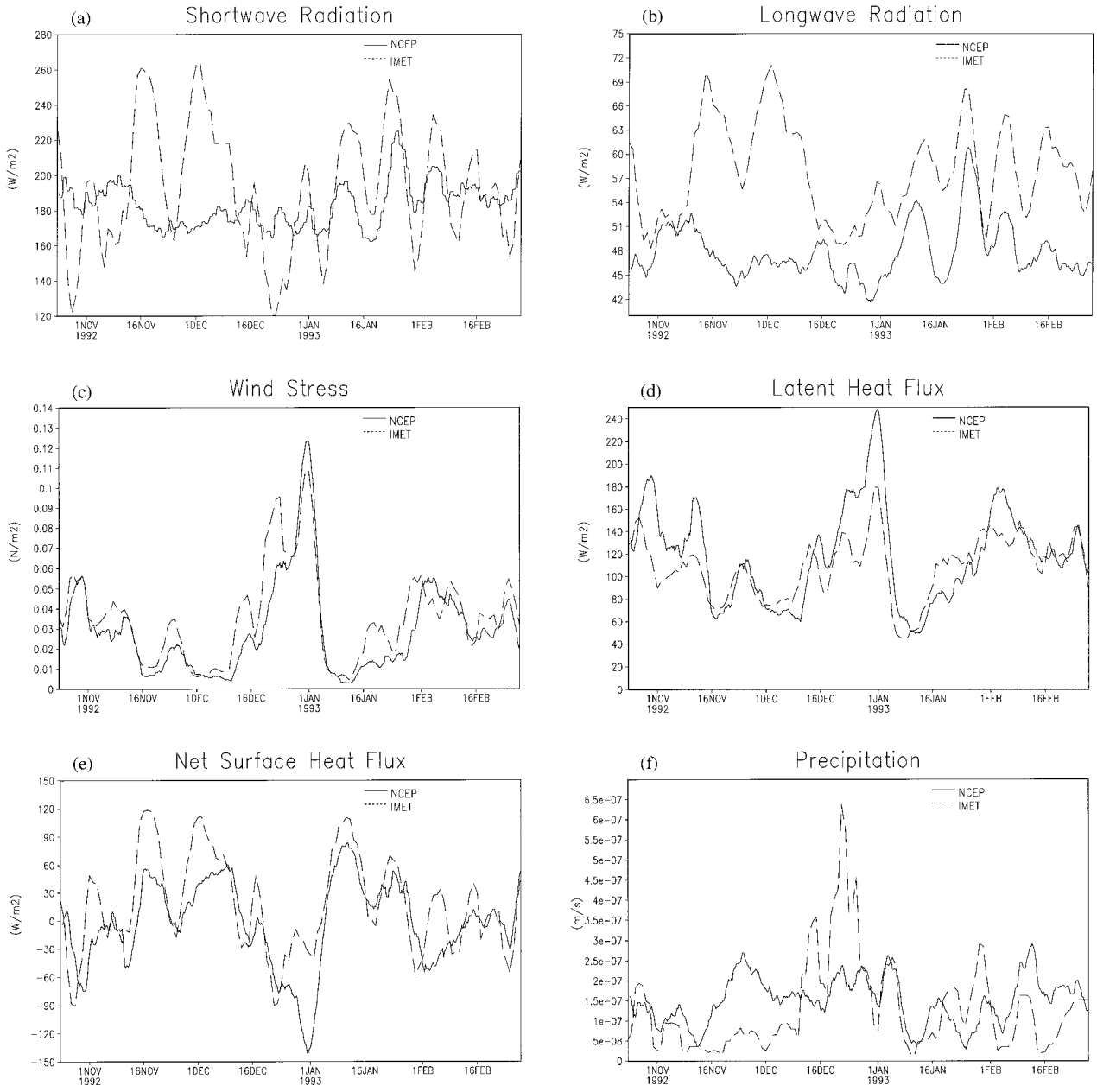

FIG. 5. Time series of (a) shortwave radiation, (b) longwave radiation, (c) wind stress, (d) latent heat flux, (e) net surface heat flux, and (f) precipitation for 24 October 1992–28 February 1993. Dashed lines indicate flux estimates from the IMET mooring observations at 1°45′S, 156°E. Thick lines indicate fluxes from NCEP reanalyses at 2.5°S, 155°E. A 5-day running average was applied to all time series.

variation from the NCEP reanalyses is slightly larger compared to the estimate from the Berliand and Berliand (1952) formula (see also Fig. 4e), whereas the phase agrees well (minimum cooling near −100°). The mean NCEP longwave cooling, however, is some 10–15 W m^{-2} lower. The NCEP wind stress (Fig. 7c) and latent heat flux (Fig. 7d) agree well, in both phase and amplitude, with the estimates based on ECMWF wind. However, the NCEP latent heat flux is lower by about 15 W m^{-2} during the period of strong wind. The net surface heat flux variation is shown in Fig. 7e. The amplitude of intraseasonal variation of the NCEP net surface flux is significantly smaller than the estimate based on SHG98, mainly because of the deficient variation of the NCEP shortwave radiation. A lower mean net longwave cooling from the NCEP reanalyses also contributes to a larger composite mean net surface heat flux.

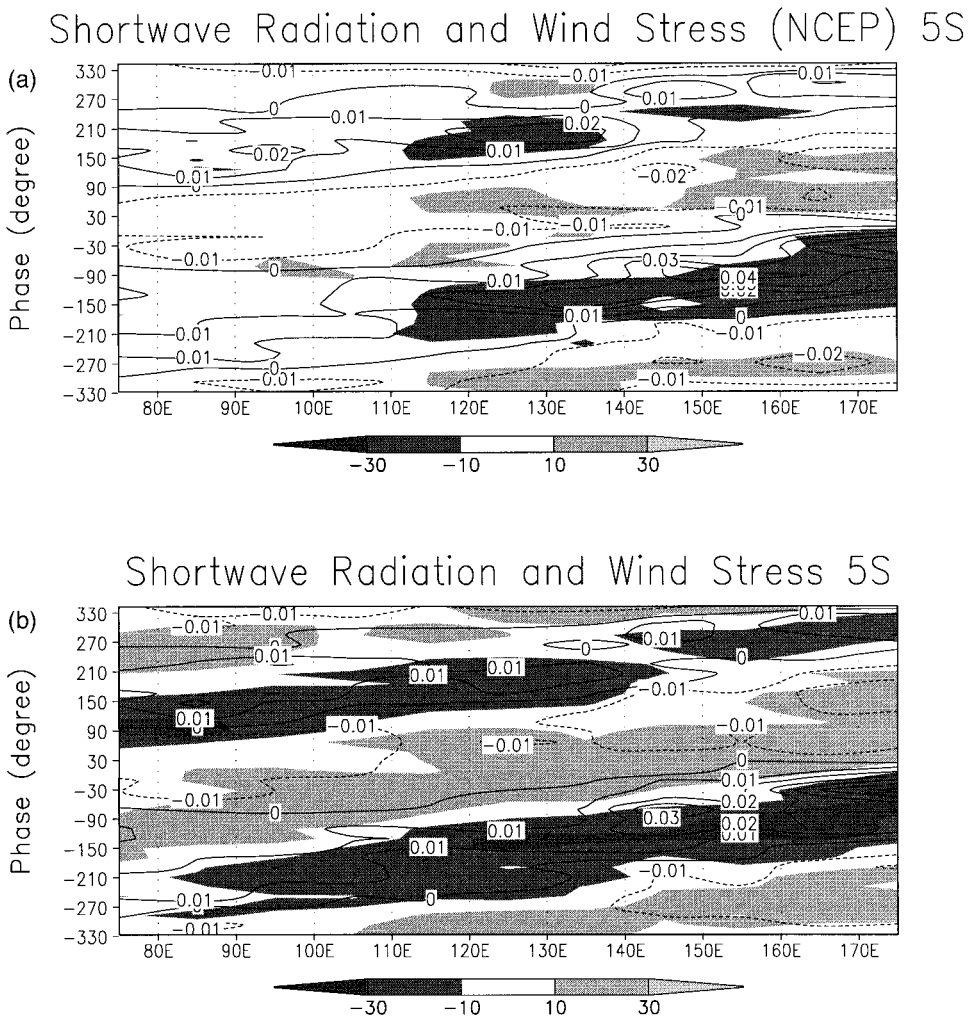

FIG. 6. Composite shortwave radiation anomaly (shading) and zonal stress (contours) from (a) NCEP reanalyses and (b) estimates described in SHG98 for the 10 MJO events defined by SHG98. The vertical axis indicates the phase based on the EOFs of OLR (see text). One cycle is approximately 50 days. The contour interval for stress is 0.01 N m^{-2} and the shading levels for shortwave radiation are 20 W m^{-2} with the first shade at +10 and −10 W m^{-2}. Linear trends along the vertical axis are removed.

The composite precipitation from the NCEP reanalyses and from the MSU are shown in Fig. 7f. Although a slight intraseasonal variation, with correct phase, is evident in the NCEP reanalyses, the peak amplitude during the windy/wet phase of MJO (near −100° and +300°) is only about half that from the MSU. Again, deficiencies in the depiction of intraseasonal convective activity by the NCEP reanalysis model appear to account for the majority of the differences between these flux variations over the life cycle of the MJO.

4. Mixed layer modeling of intraseasonal SST variability

Previously, Shinoda and Hendon (1998) showed that a one-dimensional mixed layer model is able to simulate the observed intraseasonal SST variation in the warm pool reasonably well using the surface flux estimates by SHG98. Further insight into the reliability of the intraseasonal surface fluxes from the NCEP reanalyses is provided by driving a mixed layer model with the MJO composite surface fluxes and comparing the resultant mixed layer temperature variation to the observed SST variation and the model SST from the experiment forced with surface flux estimates by SHG98. The mixed layer model is also integrated during COARE, so that comparison can be made to the model forced with the accurate IMET fluxes.

The one-dimensional model used here is that of Price et al. (1986, hereafter PWP model). The time interval of surface fluxes used for the experiments during the COARE period is 6 h. Daily mean surface heat, mo-

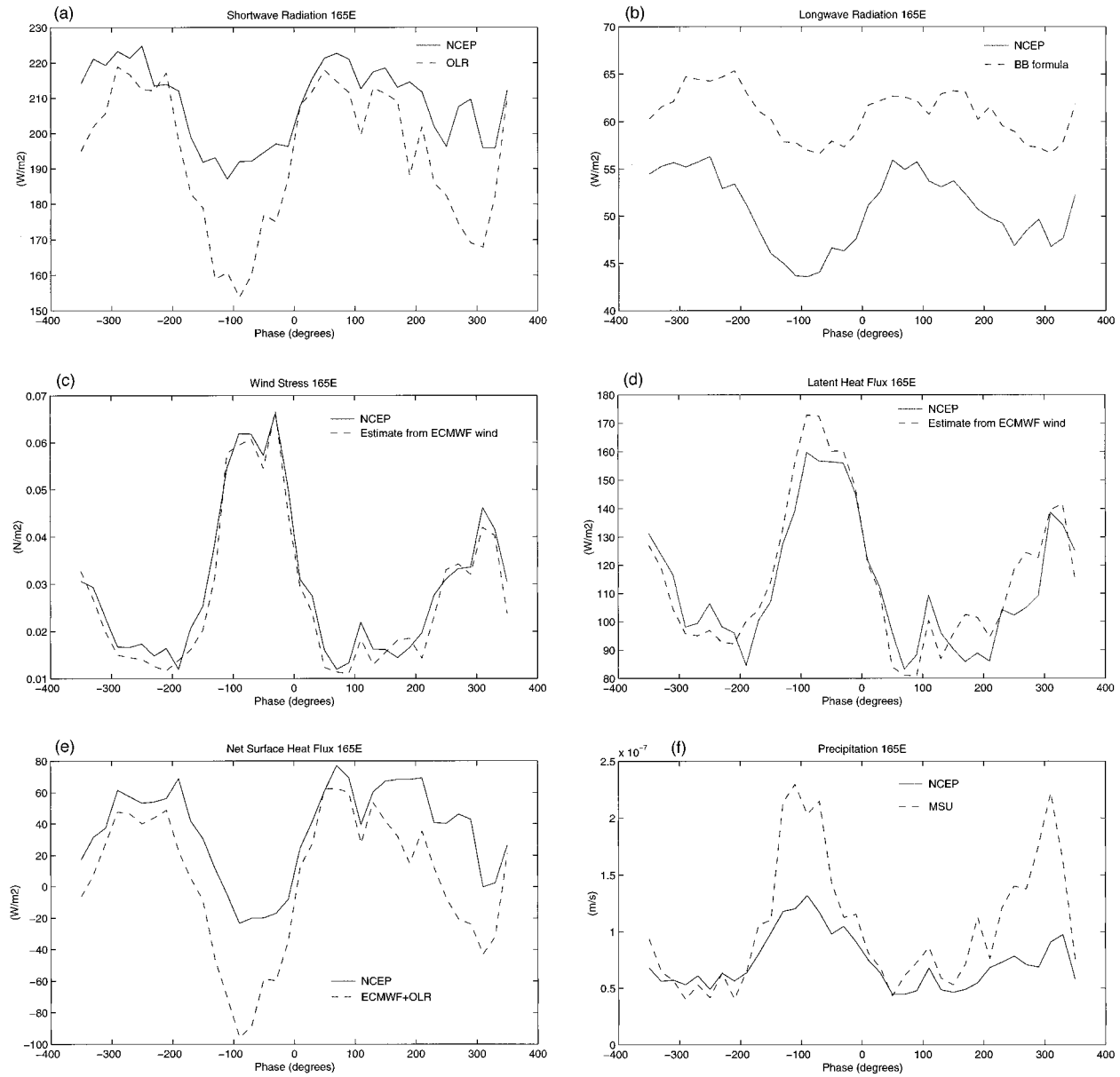

FIG. 7. Composite (a) shortwave radiation, (b) longwave radiation, (c) wind stress, (d) latent heat flux, (e) net surface heat flux, and (d) precipitation for 10 MJO events (defined by SHG98) at 2.5°–7.5°S, 160°–170°E. The horizontal axis indicates the phase based on the EOFs of OLR (see text). Thick curves indicate fluxes from NCEP reanalyses. Dashed curves indicate flux estimates by SHG98.

mentum, and freshwater fluxes are used for the composite MJO cases. An idealized diurnal cycle of shortwave radiation is included for the composite MJO as in Shinoda and Hendon (1998). Annual-mean climatological profiles of temperature and salinity (Levitus et al. 1994; Levitus and Boyer 1994) are used for the initial conditions. The *e*-folding scale of the absorption of shortwave radiation is 20 m for the fairly clear water (type 1A) in the western Pacific, and 62% of shortwave radiation is absorbed at the surface (Paulson and Simpson 1977). Details of the model integration are found in Shinoda and Hendon (1998).

a. TOGA COARE

The COARE-mean (22 October 1992–2 March 1993) net surface heat flux at 2.5°S, 155°E from the NCEP reanalyses is 19 W m^{-2} smaller than that from the IMET mooring. This difference in net surface heat flux affects the amplitude of intraseasonal SST variation because the mean mixed layer depth changes in response to the mean net surface heat flux (e.g., a larger mean net surface heat flux leads to a shallower mean mixed layer depth and hence larger intraseasonal SST variations due to the smaller heat capacity of the shallower mixed lay-

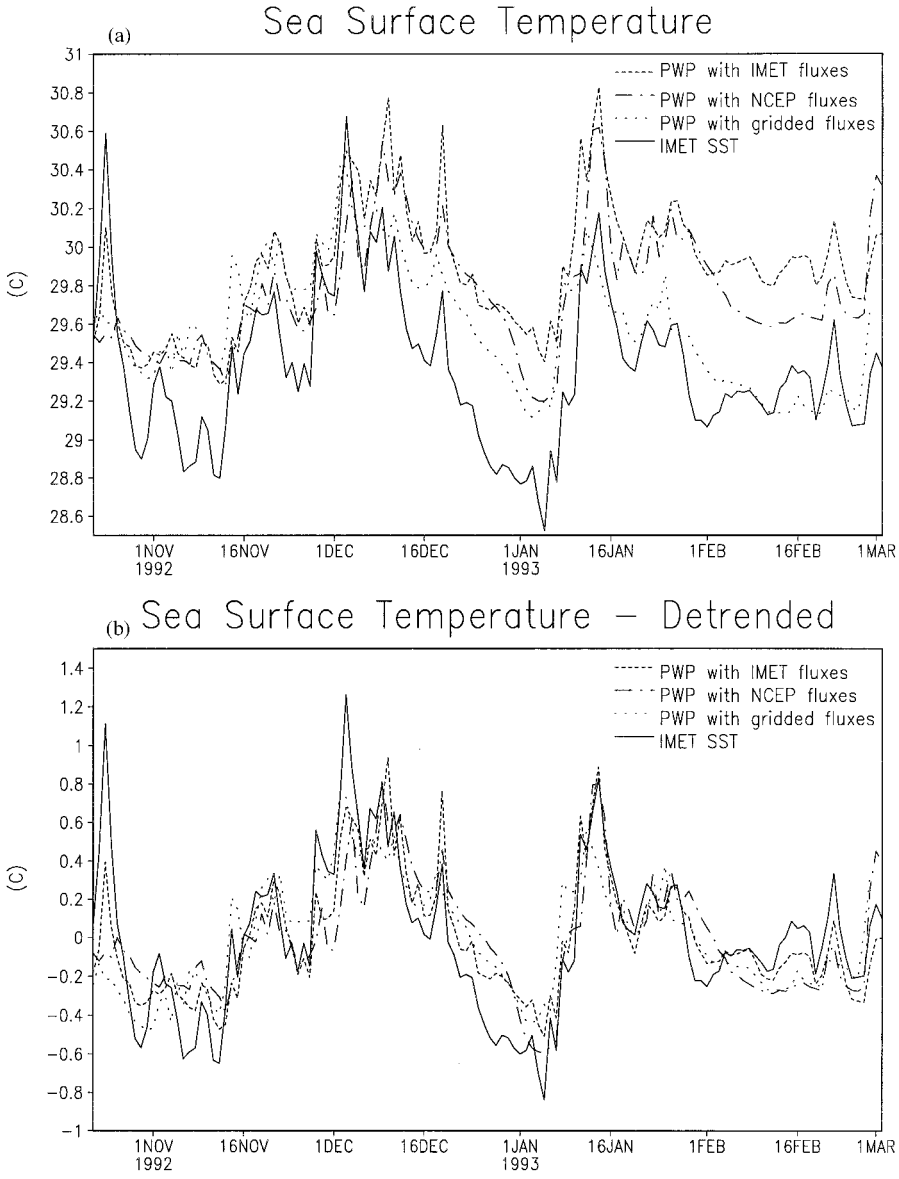

FIG. 8. (a) Time series of daily mean SST from the mixed layer model and observation at 1°45′S, 156°E for 22 October 1992–2 March 1993. The dashed curve indicates SST from the PWP model with surface fluxes estimated from the IMET observations. The dotted curve indicates SST from the PWP model with surface fluxes estimated by Shinoda and Hendon (1997). The dash–dotted curve indicates SST from the PWP model with surface fluxes from the NCEP reanalyses. The thick curve indicates SST observed at the IMET mooring. (b) Same as (a) except linear trends are removed and means are subtracted.

er). To remove the effect of the mean heat flux difference, constant values of each component heat flux are added so that the mean of each flux is the same as that of the IMET estimates. Note that the freshwater flux from NCEP reanalyses is not adjusted.

Time series of the observed SST variation at the IMET mooring and from the mixed layer model experiments are shown in Fig. 8. The SST at 0.45-m depth from the IMET mooring is used. The model SST is taken to be the mixed layer temperature. The model SST, forced with NCEP fluxes and with the IMET fluxes, reasonably depicts the observed intraseasonal SST variation; however, a significant cooling trend in late December in the observed SST is not captured by the model. Ralph et al. (1997) diagnosed this cooling trend to be due to episodic cold advection, which of course, is not included in the one-dimensional model runs (see also Feng et al. 1998). Also shown in Fig. 8a is the SST from the model forced with the fluxes from Shinoda and Hendon (1998). In this run, the model SST is used in

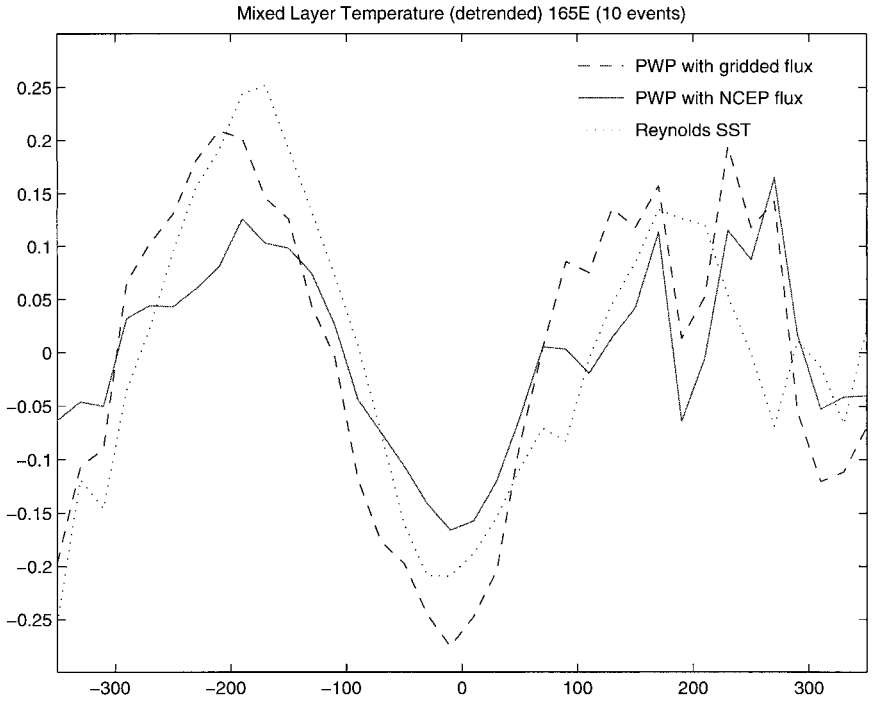

FIG. 9. Composite SST anomalies from the mixed layer model and observations (Reynolds and Smith 1994) at 2.5°–7.5°S, 160°–170°E for the 10 MJO events defined by SHG98. The thick curve indicates SST anomalies from the PWP model forced with NCEP surface fluxes. The dashed curve indicates SST anomalies from the PWP model forced with surface fluxes estimated by SHG98. The dotted curve indicates the weekly SST anomalies from observations (Reynolds and Smith 1994). Linear trends are removed.

the calculation of the latent and sensible heat fluxes and in the longwave cooling, which acts to reduce the net surface heat flux (i.e., the mean for this run is 2 W m^{-2}, which is some 16 W m^{-2} smaller than mean net heat flux from the IMET data). The result of this reduced mean net heat flux is that the SST exhibits less positive trend over the course of the integration. Nonetheless, the intraseasonal variations are similar in all three runs, including the underestimation of the the cooling tendency in late December. Removal of the trend from all four time series (Fig. 8b) highlights the good agreement of the three model runs.

Shinoda and Hendon (1998) indicated that the intraseasonal SST variation is mainly determined by the summation of the intraseasonal shortwave radiation and latent heat flux variations. The results of the current experiments are consistent with that of Shinoda and Hendon (1998) since the intraseasonal variation of net surface heat flux from NCEP reanalyses agrees reasonably well with the IMET and Shinoda and Hendon (1998) estimates (Fig. 7e). However, the agreement for the NCEP reanalyses is partially due to the cancellation of an overestimated latent heat flux and an underestimated shortwave radiation flux at the IMET site during COARE (see section 3). Also, the surface buoyancy flux due to the error of precipitation could be partially cancelled by the error of the net surface heat flux from the NCEP analyses. For instance, the observed heavy precipitation during late December is underestimated in the NCEP analyses and it may reduce the subsequent warming in early January, whereas the more rapid increase of the net surface heat flux in NCEP analyses in early January may enhance the warming.

b. Composite MJO

Not all of the variability at the IMET site during COARE can be attributed to the MJO. In an endeavor to quantify the ability of the NCEP fluxes to reproduce the SST variability due solely to the MJO, the mixed layer model is integrated for each of the 10 MJO events identified by SHG98 and the resulting output averaged for the 10 events. As for the runs during COARE, the NCEP heat fluxes are adjusted by adding constant values to each component so that the mean values for the composite are the same as those estimated by SHG98.

The composite SSTs for the grid box centered at 5°S, 165°E are shown in Fig. 9 for the observed SST (Reynolds and Smith 1994), the model forced with NCEP fluxes, and the model forced with fluxes from SHG98. To emphasize the intraseasonal variations, the mean and linear trend along the phase axis are removed. The amplitude of the model SST anomaly forced by NCEP fluxes is about 0.14°C, whereas that from the SHG98

fluxes and the observations is about 0.24°C. Thus, the intraseasonal SST fluctuations driven by NCEP surface fluxes is 30%–40% smaller than observed or than that driven by the SHG98 fluxes. This underestimation using NCEP fluxes holds true at other points across the warm pool (not shown). At 165°E the underestimation by the NCEP reanalyses of the intraseasonal variation of shortwave radiation by about 50% results in an underestimation of the intraseasonal SST variations by about 0.1°C. These results also indicate that the apparently good simulation with the NCEP fluxes at the IMET site during COARE (Fig. 8) is not representative of other MJO events.

Although this SST difference of 0.1°C is significant compared to the intraseasonal SST amplitude of 0.25°C, it is relatively small compared to the interannual SST variation in this region. However, this small difference can have an important effect since the MJO is a large-scale phenomenon. The spatial coherence of the SST variation associated with MJO is ≈8000 km zonally and ≈1500 km meridionally (e.g., Hendon and Glick 1997; SHG98). When the convective disturbance is located in the Indian Ocean, the entire equatorial Indian Ocean cools and the western Pacific warms, and one-half cycle later (≈25 days), the equatorial Indian Ocean cools and western Pacific warms. This large-scale feature of SST anomalies suggests that even such a small difference of SST associated with MJO has potentially large impact on the air–sea interaction processes in the warm pool and thus the global atmospheric circulation.

Although the comparison of the model SST with the observed SST suggests that the model simulation with NCEP fluxes underestimates the intraseasonal SST amplitude, it is still uncertain whether the 0.1°C difference is within the error of SST weekly analyses. SHG98 compared the SST weekly analyses with TAO mooring data in the western Pacific during October 1992–July 1993. The result suggests that the weekly SST analyses are reliable for accurately capturing the large intraseasonal events. However, further comparison in different locations and time periods is necessary to determine the accuracy of SST weekly analyses for this timescale.

5. Conclusions

Reanalysis of meteorological fields by NCEP, in conjunction with NCAR, has provided 40 yr of homogeneous data, with no spurious discontinuities due to changes in the assimilation model or scheme. Together with standard meteorological fields such as winds and temperatures, the NCEP reanalyses also provide a complete suite of surface fluxes, which have many potential usages, especially in the realm of ocean general circulation modeling. These fluxes are, however, not directly observed or assimilated and hence are strongly dependent on the physical parameterizations in the assimilation model. Despite the fact that they are internally consistent with the analyzed circulation produced by the assimilation model, the reanalyzed surface fluxes may not necessarily accurately reflect reality. Thus, assessment of the reliability of the surface fluxes from the reanalyses is required.

The present study focused on the depiction of intraseasonally varying surface fluxes across the warm pool of the Indian and western Pacific Oceans by the NCEP reanalyses. Particular emphasis was given to the surface fluxes produced by the MJO, as this is the dominant mode of large-scale intraseasonal variability across the warm pool. The potential role of air–sea interaction associated with such intraseasonal variability for the maintenance (e.g., Ralph et al. 1997) and interannual variation (e.g., Kessler et al. 1995) of the warm pool provides impetus for this investigation.

The magnitude, spatial distribution, and coherence of the intraseasonal surface fluxes from the NCEP reanalyses were compared to various gridded estimates produced by SHG98 for the period 1986–93. The estimates of SHG98 were derived from a combination of independent observations (e.g., MSU rainfall and satellite observed OLR), ECMWF uninitialized wind and surface pressure analyses, and empirical bulk formulas. In general, the agreement for surface winds and stress was much better than for fluxes that depend strongly on convective variability, such as freshwater flux, surface shortwave and longwave radiation, and to a lesser degree, latent heat flux. In particular, the NCEP reanalyses appears to reasonably capture the spatially coherent variations in surface winds produced by the MJO. However, the comparison of the distribution of intraseasonal rainfall and its coherence with MSU rainfall, along with a similar comparison between NCEP OLR and observed OLR, indicates that intraseasonal convective activity, while exhibiting some semblance of realistic coherent eastward propagation, is underestimated in the NCEP reanalyses by more than a factor of 2.

Comparison was also made to the intraseasonal surface flux variations observed at the IMET mooring (1°45′S, 156°E) during COARE (22 October 1992–2 March 1993; Weller and Anderson 1996). Whereas the NCEP intraseasonal surface stress variation was in close agreement with that at the IMET mooring, almost no signal of the large MJO events that traversed the mooring was evident in the NCEP surface shortwave and longwave radiation. Furthermore, the mean NCEP longwave cooling during COARE was some 10–15 W m^{-2} less than observed at the IMET mooring. Interestingly, the NCEP longwave cooling estimates appear most deficient at times of strongest intraseasonal cooling, when cloud cover is at a minimum and surface shortwave radiation is a maximum. This indicates that the production of overly constant intraseasonal convection in the NCEP reanalyses also adversely impacts the mean longwave cooling over the warm pool.

The present results suggest that intraseasonal variation of surface radiation and precipitation from the NCEP re-

analyses are not reliable across the warm pool. These variables strongly depend on convection and associated cloudiness. Weare (1997) suggested that the primary error of the shortwave radiative forcing is due to too reflective clouds in the NCEP analyses. However, the present results suggest that on intraseasonal timescales, the problem is primarily in the lack of coherent variability.

The impact of the underestimation of intraseasonal variations of surface radiation and precipitation on intraseasonal SST variability in the warm pool was explored with a one-dimensional mixed layer model. During COARE, the intraseasonal SST variability in the model driven by the NCEP surface fluxes agrees well with both the model SST driven by IMET fluxes and the observed SST variability. However, this result appears to be somewhat fortuitous, as the NCEP reanalyses appear to overestimate the magnitude of the intraseasonal latent heat flux variation during COARE at the IMET site. This overestimation of the latent heat flux variation compensates for the underestimation of surface shortwave radiation variation. When the model is forced with the surface heat flux variations from NCEP for 10 well-defined MJO events, the amplitude of the SST variation is about 30%–40% smaller than observed or from the model when driven by the fluxes from SHG98. This reduced amplitude is primarily caused by the underestimation of shortwave radiation variations in the NCEP reanalyses.

On a hopeful note, the NCEP reanalyses do depict some semblance of the coherent convective variability associated with the MJO across the warm pool. Although the amplitude of this variability in precipitations, shortwave radiation, and OLR is too weak by at least a factor of 2, it does show some coherence with the observed variability, as depicted by MSU precipitation and satellite-observed OLR. The appearance of such realistic coherent structure presumably results from the physical parameterizations in the assimilation model responding to the presence of the MJO in large-scale dynamical fields, such as zonal wind, which appear to be well depicted in the reanalyses. Future reanalysis efforts could thus seem to benefit from improvements in the parameterization of large-scale convection or from direct assimilation of some measure of large-scale convection.

Acknowledgments. The SRB data were obtained from the NASA/Langley Research Center EOSDIS Distributed Active Archive Center. Robert Weller kindly provided us with the WHOI IMET mooring data. We acknowledge constructive comments from the two anonymous reviewers. This work was supported by a TOGA COARE grant from NOAA's Office of Global Programs.

REFERENCES

Bony, S., Y. Sud, K. M. Lau, J. Susskind, and S. Saha, 1997: Comparison and satellite assessment of NASA/DAO and NCEP–NCAR reanalyses over tropical ocean: Atmospheric hydrology and radiation. *J. Climate,* **10,** 1441–1462.

Berliand, M. E., and T. G. Berliand, 1952: Determining the net longwave radiation of the earth with consideration of the effect of cloudiness (in Russian). *Izv. Akad. Nauk SSSR, Ser. Geofiz.,* **1**.

Fairall, C., E. F. Bradley, D. P. Rogers, J. B. Edson, and G. S. Young, 1996: The TOGA COARE bulk flux algorithm. *J. Geophys. Res.,* **101,** 3747–3764.

Feng, M., P. Hacker, and R. Lukas, 1997: Upper ocean heat and salt balances in response to a westerly wind burst in the western equatorial Pacific. *J. Geophys. Res.,* **103,** 10 289–10 311.

Gruber, A., and A. F. Krueger, 1984: The status of the NOAA outgoing longwave radiation data set. *Bull. Amer. Meteor. Soc.,* **65,** 958–962.

Gutzler, D. S., G. N. Kiladis, G. A. Meehl, K. M. Weickmann, and M. Wheeler, 1994: The global climate of December 1992–February 1993. Part II: Large-scale variability across the tropical western Pacific during TOGA COARE. *J. Climate,* **7,** 1606–1622.

Hendon, H. H., and J. Glick, 1997: Intraseasonal air–sea interaction in the tropical Indian and Pacific Oceans. *J. Climate,* **10,** 647–661.

Kalnay, E., and Coauthors, 1996: The NCEP/NCAR 40-Year Reanalysis Project. *Bull. Amer. Meteor. Soc.,* **77,** 437–471.

Kessler, W. S., M. J. McPhaden, and K. M. Weickmann, 1995: Forcing of intraseasonal Kelvin waves in the equatorial Pacific Ocean. *J. Geophys. Res.,* **100,** 10 613–10 631.

Lau, K.-M., and C.-H. Sui, 1997: Mechanisms of short-term sea surface temperature regulation: Observations from TOGA COARE. *J. Climate,* **10,** 465–472.

Levitus, S., and T. P. Boyer, 1994: *World Ocean Atlas.* Vol. 4, *Temperature,* NOAA, 117 pp.

——, R. Burgett, and T. P. Boyer, 1994: *World Ocean Atlas.* Vol. 3, *Salinity,* NOAA, 97 pp.

Li, Z., and H. G. Leighton, 1993: Global climatologies of solar radiation budgets at the surface and in the atmosphere from 5 years of ERBE data. *J. Geophys. Res.,* **98,** 4919–4930.

Liebmann, B., and C. A. Smith, 1996: Description of a complete (interpolated) outgoing longwave radiation dataset. *Bull. Amer. Meteor. Soc.,* **77,** 1275–1277.

Madden, R. A., and P. R. Julian, 1971: Detection of a 40–50 day oscillation in the zonal wind in the tropical Pacific. *J. Atmos. Sci.,* **28,** 702–208.

——, and ——, 1972: Description of global-scale circulation cells in the Tropics with a 40–50 day period. *J. Atmos. Sci.,* **29,** 1109–1123.

Paulson, C. A., and J. J. Simpson, 1977: Irradience measurements in the upper ocean. *J. Phys. Oceanogr.,* **7,** 952–956.

Pinker, R., and I. Laszlo, 1992: Modeling of surface solar irradiance for satellite applications on a global scale. *J. Appl. Meteor.,* **31,** 194–211.

Price, J. F., R. A. Weller, and R. Pinkel, 1986: Diurnal cycling: Observations and models of the upper ocean response to diurnal heating, cooling, and wind mixing. *J. Geophys. Res.,* **91** (C7), 8411–8427.

Ralph, E. A., K. Bi, and P. P. Niiler, 1997: A Lagrangian description of the western equatorial Pacific response to the wind burst of December 1992. *J. Climate,* **10,** 1706–1721.

Reynolds, R. W., and T. M. Smith, 1994: Improved global sea surface temperature analyses using optimum interpolation. *J. Climate,* **7,** 929–948.

Rossow, W. B., and R. A. Schiffer, 1991: ISCCP cloud data products. *Bull. Amer. Meteor. Soc.,* **72,** 2–20.

Salby, M. L., and H. H. Hendon, 1994: Intraseasonal behavior of clouds, temperature, and motion in the Tropics. *J. Atmos. Sci.,* **51,** 2207–2224.

Shinoda, T., and H. H. Hendon, 1998: Mixed layer modeling of intraseasonal variability in the tropical western Pacific and Indian Oceans. *J. Climate,* **11,** 2668–2685.

——, ——, and J. Glick, 1998: Intraseasonal variability of surface

fluxes and sea surface temperature in the tropical western Pacific and Indian Oceans. *J. Climate,* **11,** 1685–1702.

Spencer, R. W., 1993: Global oceanic precipitation from the MSU during 1979–91 and comparisons to other climatologies. *J. Climate,* **6,** 1301–1326.

Waliser, D. E., and N. E. Graham, 1993: Convective cloud systems and warm-pool sea surface temperatures: Coupled interactions and self-regulation. *J. Geophys. Res.,* **98** (D7), 12 881–12 893.

Weare, B. C., 1997: Comparison of NCEP–NCAR cloud radiative forcing reanalyses with observations. *J. Climate,* **10,** 2200–2209.

Webster, P. J., and R. Lukas, 1992: The Tropical Ocean Global Atmosphere Coupled Ocean–Atmosphere Response Experiment (COARE). *Bull. Amer. Meteor. Soc.,* **73,** 1377–1416.

Weller, R. A., and S. P. Anderson, 1996: Surface meteorology and air–sea fluxes in the western equatorial Pacific warm pool during the TOGA Coupled Ocean Atmosphere Response Experiment. *J. Climate,* **9,** 1959–1990.

Whitlock, C. H., and Coauthors, 1995: First Global WCRP shortwave surface radiation budget dataset. *Bull. Amer. Meteor. Soc.,* **76,** 905–922.

Zeng, X., M. Zhao, and R. E. Dickinson, 1998: Intercomparison of bulk aerodynamic algorithms for the computation of sea surface fluxes using the TOGA COARE and TAO data. *J. Climate,* **11,** 2628–2644.

Zhang, C., 1996: Atmospheric intraseasonal variability at the surface in the tropical western Pacific Ocean. *J. Atmos. Sci.,* **53,** 739–758.